Journal of Applied Polymer Science

# Online monitoring of drop/particle size and size distribution in liquid–liquid dispersions and suspension polymerizations by optical reflectance measurements

**Guiming Xie, Pengju Pan, Yongzhong Bao**
State Key Laboratory of Chemical Engineering, College of Chemical and Biological Engineering, Zhejiang University, Hangzhou 310027, China
Correspondence to: Y. Bao (E-mail: yongzhongbao@zju.edu.cn)

**ABSTRACT:** Evolutions of drop/particle size and size distribution in liquid–liquid dispersions and suspension polymerizations of methyl methacrylate (MMA) were monitored by using an online optical reflectance measurement (ORM), and effects of operating parameters such as the agitation rate, concentration of poly(vinyl alcohol) (PVA) dispersant, and initial concentration of poly(methyl methacrylate) (PMMA) in MMA monomer on the Sauter mean diameter ($d_{32}$) and size distribution of drop/particle were investigated. According to the variations of $d_{32}$ of drops/particles with time, four characteristic particle formation stages can be identified for suspension polymerization process. The factors that lead to increase the rate of drop break up, such as increasing of concentration of PVA and decreasing of viscosity of dispersed phase, would postpone the particle growth stage. The $d_{32}$ and size distribution breadth of drops/particles were significant increased when the liquid–liquid dispersions or suspension polymerizations were conducted at low PVA concentrations or MMA/PMMA solutions with high PMMA contents were used as the dispersed phase, in consistent with the scanning electron micrograph observation on final PMMA particles. It is clear that ORM can be effectively applied in online monitoring of size and size distribution of drops/particles in the liquid–liquid dispersions and suspension polymerizations. © 2016 Wiley Periodicals, Inc. J. Appl. Polym. Sci. **2016**, *133*, 43632.

**KEYWORDS:** kinetics; morphology; radical polymerization

Received 22 November 2015; accepted 9 March 2016
**DOI: 10.1002/app.43632**

## INTRODUCTION

Suspension polymerization has been widely used to produce poly(vinyl chloride), vinylidene chloride copolymers, polystyrene, poly(methyl methacrylate), and high value-added polymer particulate products (e.g., chromatographic separation media, ion exchange resins, and enzyme immobilization supports).[1–3] During the suspension polymerization process, a monomer (or monomers) that is immiscible or slightly soluble in water is first dispersed to form the monomer drops by stirring in the aqueous phase containing a dispersant. The polymerization starts when the monomer(s) in the separated drops is initiated by an oil-soluble initiator. Then, the monomer drops will gradually transfer from pure monomer drops to the viscous polymer/monomer solution drops or monomer-contained polymer particles, and finally to polymer particles, depending on the solubility between monomer(s) and its polymer. The coalescence of dispersed drops is often occurred as the viscosity of dispersed phase is increased with the increase of monomer(s) conversion.[1–3] Therefore, the mean size, size distribution, and morphology of synthesized polymer particles, which are key factors influencing the quality of polymer products, are always correlated with the dynamic equilibrium between the drop breakage and coalescence, which depends on the operating conditions such as the geometry of reactor and agitator, properties of dispersed and continuous phases, interfacial tension, agitation rate, and polymerization conversion.

Because the viscoelastic properties of dispersed phase and the dynamic equilibrium between breakage and coalescence of drops/particles are varied in the polymerization process, the quantitative analysis of drop/particle size and size distribution in suspension polymerization is rather difficult. Most of previous studies have been focused on the liquid–liquid dispersion with a dilute, nonviscous, and nonreactive dispersed phase, in which the surface force dominates stabilization of drops and the internal viscous force is negligible.[4–9] Effects of various factors such as the volume faction and viscosity of dispersed phase, type and dimension of impeller, and agitation rate on the mean drop size and size distribution have been investigated, and the

results led to the developments of models or correlations relating the Sauter mean diameter ($d_{32}$) of drops to different influencing factors. The monomer/polymer mixtures with different compositions were also used as the dispersed phase in the liquid–liquid dispersion to investigate the effects of the viscosity or conversion on the particle formation. For example, Lagisetty *et al.*[10] used the dispersed phases containing styrene and 10–30% polystyrene to investigate the influences of density and viscosity of dispersed phases on the diameter of drops. Hashim *et al.*[11,12] found that the mean drop size increased and the size distribution broadened as the concentration of dispersed phase, that is, polystyrene/styrene solution increased. Although the valid results on the evolution of drop size have been obtained, the applied experimental system was still different from the real polymerization process.

The evolution of drop/particle size and size distribution in the suspension polymerization has also been studied by several researchers using the different offline and online methods. The off-line monitoring was always carried out by withdrawing the dispersion sample from reactor at a certain time interval and giving an effective colloidal protection to drops/particles by using a concentrated solution of dispersant or emulsifier solution. The morphology and properties of drop/particle were then characterized by using either the microphotographic[13–16] or dynamic laser diffraction techniques.[17–20] Online measurement techniques used in suspension polymerization included the acoustic attenuation spectroscopy,[21] endoscope with camera,[22] stereomicroscope,[23] near infrared reflectance spectroscopy (NIRS),[24–26] and so forth. Lazrak *et al.*[27] compared the evolution of drop size for a methyl methacrylate (MMA) suspension in an aqueous agitated medium in the absence and presence of polymerization reaction by an off-line method using the dynamic laser diffraction analysis, and found that the equilibrium between coalescence and breakage was modified by the occurrence of polymerization. The evolution of mean particle size and size distribution in MMA suspension polymerization was also investigated by Jahanzad *et al.*[28,29] by using the laser diffraction analysis. Four characteristic intervals, that is, transition, quasi-steady-state, growth, and identification stages, in the evolution of particle size were identified. The influences of dispersant and initiator usages, monomer hold up, reaction temperature, and agitation speed on the characteristic intervals of the drop size as well as the polymerization kinetics were examined. Isopescu *et al.*[16] used a microscopic method to evaluate the drop/particles sizes and distribution in suspension polymerization of MMA, and a population balance model was used to describe the breakage and coalescence mechanism. Goncalves *et al.*[30] used the off-line sampling and sieving method to measure the particle size and studied the effects of reaction conditions (e.g., stirring rate, stabilizer concentration, and stabilizer addition time) on particle size in MMA suspension polymerization. Santos *et al.*[24–26] evaluated the applicability of NIRS in inline monitoring of the average particle size in the suspension polymerizations of styrene and MMA, and found that the successful implementation of NIRS greatly relied on the proper development of calibration methods with the help of both multivariate techniques and nonlinear sensor calibration models.

Based on the results of Simmons *et al.*,[31] the laser back scattering probes have been widely used in the fields such as sizing cell cultures,[32,33] nucleation or crystallization processes.[34] The techniques of focused beam reflectance measurement (FBRM) and 3D optical reflectance measurement (ORM) have been successfully applied in monitoring the dynamic solid–liquid or gas–liquid processes, crystallization processes, and liquid–liquid biocatalytic reactor.[35–38] However, the applications of FBRM and ORM techniques in the suspension polymerization are rare. Recently, Poblete *et al.*[39] employed FBRM for inline monitoring of liquid–liquid (styrene–water) dispersions and styrene suspension polymerizations and found that FBRM is capable of monitoring the initial particle breakage stage and the attainment of the final breakage/coalescence equilibrium in dispersion experiments, and coalescence stage in suspension polymerizations. However, to our knowledge, the application of ORM in suspension polymerizations has not been reported.

In this work, an online size and size distribution measurement system on ORM technique was set up to monitor the evolution of the average size and size distribution in the liquid–liquid dispersions and suspension polymerizations using MMA as a model monomer. The dispersions and suspension polymerizations were conducted at different dispersant concentrations, agitation rates, and initial viscosities of dispersed phase, to investigate their effects on drop/particles size and size distribution, and to verify the applicability of ORM on online monitoring of drop/particles sizes and size distributions at different conditions.

## EXPERIMENTAL

### Materials

MMA (analytical grades, Lingfeng Chemical, China) was distilled at reduced pressure to remove the inhibitors before use. Poly(vinyl alcohol) (PVA) with trade name GH 20 was supplied by Nippon Synthetic Chemistry and used as a dispersant. Lauroyl peroxide (LPO) (98%, Aladdin) was used as an initiator without further purification. Distilled water was used as the continuous phase.

### Liquid–Liquid Dispersion and Suspension Polymerization of MMA

The liquid–liquid dispersion and suspension polymerization experiments of MMA were carried out in a 5 L jacketed stainless-steel autoclave with an internal diameter of 14.5 cm and equipped with a single-layer inclined blade with a diameter of 7.8 cm. The temperature of vessel was controlled by pumping water with an appropriate temperature through the jacket. The agitation rate was controlled through a dimmer stat and measured through a digital tachometer connected to the stirrer shaft. An online laser particle analyzer system (Sequip IPAS, Germany) was installed on the autoclave to measure the drop/particle size and size distribution. The laser particle analyzer scene was fixed at 2 cm away from the impeller shaft with a vertical direction angle of 45°. The setup of reactor and measurement system is shown in Figure 1.

In a typical run, the autoclave was added with 2.5 L of deionized water containing PVA dispersant (1 g/L $H_2O$). The reactor

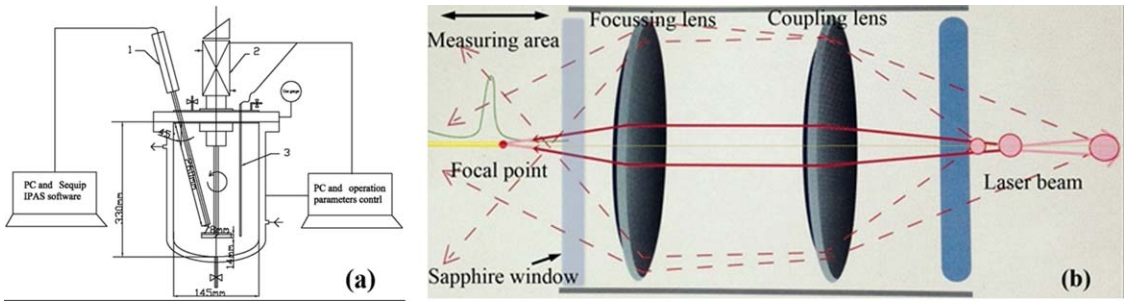


**Figure 1.** (a) Illustration of autoclave and measurement system. 1. Online laser particle size analyzer, 2. digital magnetic agitator, 3. thermocouple. (b) Principle of ORM measurement. [Color figure can be viewed in the online issue, which is available at wileyonlinelibrary.com.]

was sealed and purged by nitrogen for three times to remove the oxygen. Then, 500 g of MMA monomer with dissolved LPO (1.0 wt % based on the monomer) was added to the reactor. The liquid–liquid dispersion experiment was carried out at 30 °C with an agitation rate of 300–500 rpm. The polymerization was carried out at 70 °C after the dispersion. It was considered that the polymerization started when the temperature was raised to 70 °C.

### Measurements

The monomer conversion was calculated by gravimetric analysis of samples taken from the reactor at the desired times. The sample was poured into the ethanol containing an inhibitor (hydroquinone) and the precipitated polymer was dried to constant weight and weighed. The viscosity of PMMA/MMA solution was measured by using a rotational rheometer RS6000 at 20 °C and a shear rate of 4 $s^{-1}$. The density of PMMA/MMA solution was calculated from its volume and weight. The interfacial tension between the aqueous and oil phases was measured by a pendant drop method on an OCA 20 type instrument (Dataphysics Company, Germany) at 20 °C.

The drop/particle size and size distribution were measured by an online particle size analysis system based on ORM technique (Sequip IPAS). The laser probe is consisted of a light source and detector, and the principle of ORM measurement is also shown in Figure 1. The laser beam leaves the optical fiber, passes through the coupling lens and focusing lens, rejoins at the focal point scanning the sample in an elliptical orbit. If the laser beam hits a particle or drop at the focal point, the reflected light is then sent back to the optical fiber on the exact same path. The time interval of backward reflection would be recorded. The laser probe usually measures thousands chord length of particles per second, achieving a precise number-particle size distribution. A typical measurement is completed within several seconds, and the number of drops/particles, drop/particle size and size distribution can be obtained from the analysis system. In analyzing the particle size,[40] the density distribution is defined as:

$$q_r(x) = \frac{dQ_r(x)}{dx} \tag{1}$$

where $Q_r$ is the cumulative frequency and can be expressed as follows:

$$Q_r(x) = \frac{\text{Amount of particles} \le x}{\text{Amount of all particles}} \tag{2}$$

$Q_r(x)$ is the derivative of cumulative frequency with respect to the characteristic value $x$. $dQ_r(x)$ is dimensionless and the

**Table I.** Diameter Ranges Corresponding to the Different Channels

| Chanel | Diameter range (μm) | Channel | Diameter range (μm) | Channel | Diameter range (μm) | Channel | Diameter range (μm) |
|---|---|---|---|---|---|---|---|
| 1 | 0-0.25 | 16 | 8.74-9.97 | 31 | 51.7-57.74 | 46 | 262.88-292.58 |
| 2 | 0.25-0.53 | 17 | 9.97-11.34 | 32 | 57.74-64.46 | 47 | 292.58-325.6 |
| 3 | 0.53-0.84 | 18 | 11.34-12.86 | 33 | 64.46-71.93 | 48 | 325.6-362.31 |
| 4 | 0.84-1.18 | 19 | 12.86-14.54 | 34 | 71.93-80.24 | 49 | 362.31-403.14 |
| 5 | 1.18-1.56 | 20 | 14.54-16.42 | 35 | 80.24-89.47 | 50 | 403.14-448.54 |
| 6 | 1.56-1.99 | 21 | 16.42-18.51 | 36 | 89.47-99.74 | 51 | 448.54-499.03 |
| 7 | 1.99-2.46 | 22 | 18.51-20.84 | 37 | 99.74-111.16 | 52 | 499.03-555.17 |
| 8 | 2.46-2.99 | 23 | 20.84-23.42 | 38 | 111.16-123.86 | 53 | 555.17-617.6 |
| 9 | 2.99-3.57 | 24 | 23.42-26.29 | 39 | 123.86-137.99 | 54 | 617.6-687.02 |
| 10 | 3.57-4.22 | 25 | 26.29-29.49 | 40 | 137.99-153.69 | 55 | 687.02-764.22 |
| 11 | 4.22-4.94 | 26 | 29.49-33.04 | 41 | 153.69-171.16 | 56 | 764.22-850.06 |
| 12 | 4.94-5.75 | 27 | 33.04-36.99 | 42 | 171.16-190.57 | 57 | 850.06-945.52 |
| 13 | 5.75-6.64 | 28 | 36.99-41.38 | 43 | 190.57-212.17 | 58 | 945.52-1051.67 |
| 14 | 6.64-7.63 | 29 | 41.38-46.27 | 44 | 212.17-236.18 | 59 | 1051.67-1169.7 |
| 15 | 7.63-8.74 | 30 | 46.27-51.74 | 45 | 236.18-262.88 | 60 | 1169.7-1300.96 |

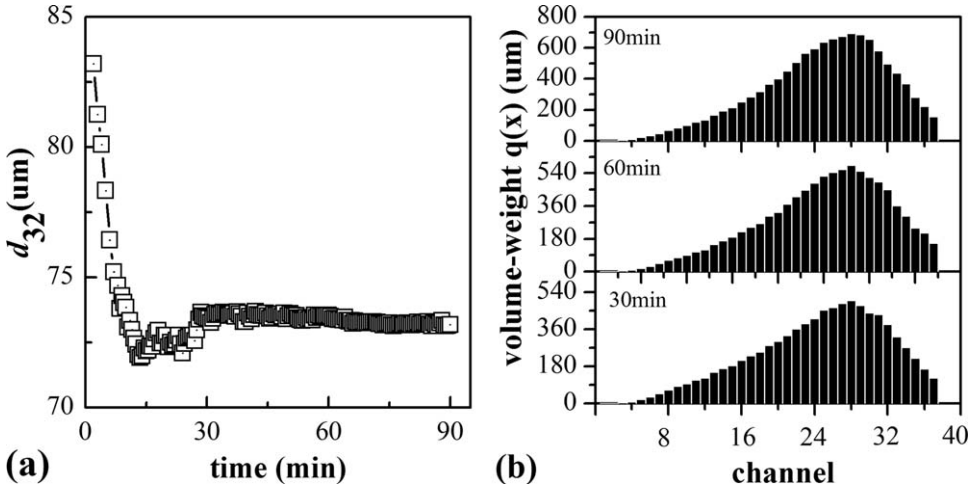


**Figure 2.** Effect of dispersion time on $d_{32}$ (a) and size distribution (b) of MMA drops at MMA/$H_2O$ = 1/5 (mass ratio), an agitation rate of 350 rpm, and a PVA concentration of 1.0 g/L $H_2O$.

ordinate $Q_r(x)$ has the dimension of $\mu m^{-1}$. The diameter ranges corresponding to different channels are shown in Table I.

The morphology of polymer particles was observed using a CARL ZEISS ULTRA 55 scanning electron microscope (SEM). The sample was coated with a thin layer of gold prior to analysis.

## RESULTS AND DISCUSSION

### Online Monitoring of Drop Size and Size Distribution in Liquid–Liquid Dispersions

The influence of dispersion time on drop size and size distribution was studied to determine the dispersion time for obtaining a stable dispersion. Figure 2 shows the variations of Sauter mean diameter ($d_{32}$) and size distributions with the dispersion time at a fixed dispersion composition and an agitation rate of 350 rpm.

It can be seen that the drop size is rapidly decreased and the size distribution is obviously changed with time at the early dispersion stage. A balanced state is achieved as the dispersion time exceeds 30 min. These profiles are in agreement with the results reported by Lazrak[27] and Hashim.[11] Under the turbulent flow conditions, the size of drops is the result of a balance between the rates of breakup and coalescence. The coalescence of drops is more complex than the breakup since it involves not only the approach of two drops but also the drainage and eventual rupture of the intervening liquid film, in which the physical properties of fluids and interfaces play an important role. As the dispersion proceeds, the physical properties of dispersed and continuous phases change little, while the interface properties would gradually vary as the added PVA dispersant molecules are adsorbed onto the interface of drops, rearrange themselves and prevent the drop from coalescence.[41] When the absorption of PVA reaches an equilibrium state, the dynamic equilibrium between the breakup and coalescence would also be attained, and the size and size distribution of drops would change no more with the further increasing of dispersion time. Thus, the dispersion time was set to be 30 min for studying the effects of polymerization conditions on the average size and size distribution of drops.

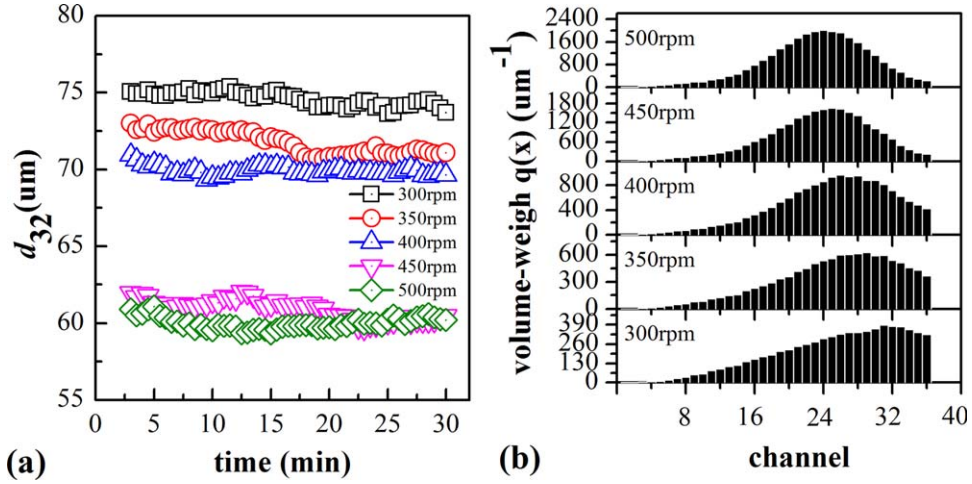


**Figure 3.** Influence of agitation rate on $d_{32}$ (a) and size distribution (b) of MMA drops at MMA/$H_2O$ = 1/5 (mass ratio) and a PVA concentration of 1.0 g/L $H_2O$. [Color figure can be viewed in the online issue, which is available at wileyonlinelibrary.com.]

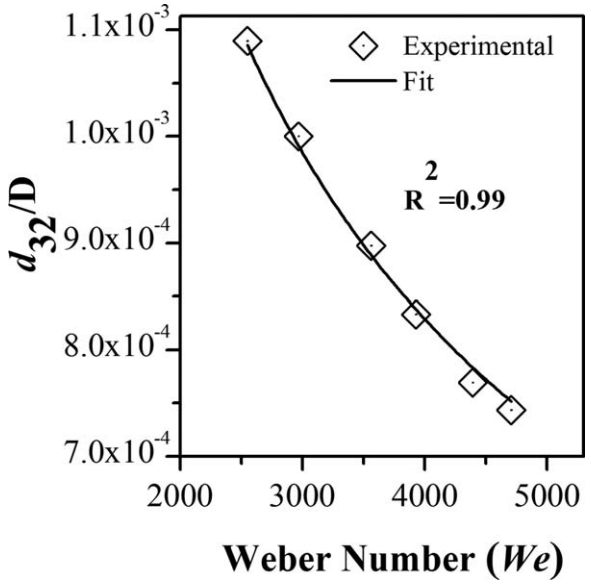


**Figure 4.** Variation of $d_{32}$/D with *We*.

Figure 3 illustrates the effect of agitation rate on $d_{32}$ and size distribution of MMA drops. It can be seen that $d_{32}$ decreases and the size distribution becomes narrow as the agitation rate increases from 300 to 500 rpm. The increase of agitation rate induces a higher breakage frequency and thus favors the formation of smaller drops.

Variation of the dimensionless size ratio ($d_{32}/D$) with the dimensionless Weber number (*We*) is shown in Figure 4.

The following equation is obtained by no-linear fitting of the results shown in Figure 4.

$$\frac{d_{32}}{D} = K_1(0.06 + K_2\varphi)We^{-n} = 0.06(1 + 5\varphi)We^{-0.6} \quad (3)$$

The exponent of *We* is consistent with the reported values,[19,27,42–46] and the values of $K_1$ and $K_2$ are in the range reviewed by Zhou.[42]

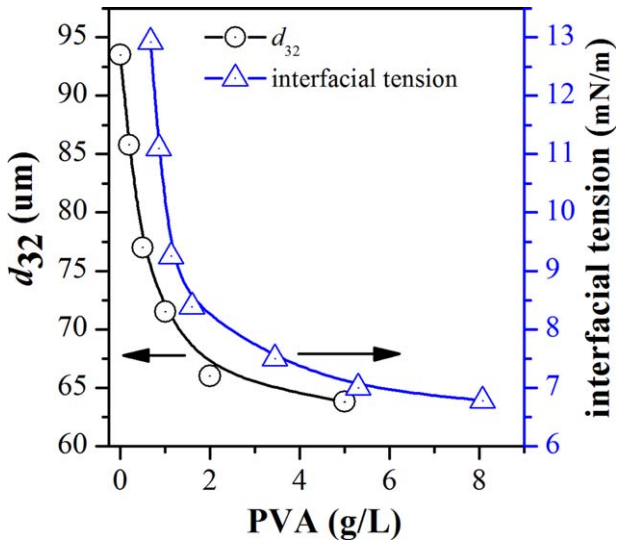


**Figure 6.** Variation of $d_{32}$ (at an agitation rate of 350 rpm) and interfacial tension between aqueous and monomer phases with PVA concentration. [Color figure can be viewed in the online issue, which is available at wileyonlinelibrary.com.]

The dispersant or stabilizer plays an important role in the stabilization of drops/polymer particles in suspension polymerization. Effects of PVA dispersant concentration on $d_{32}$ and size distribution of MMA drops are shown in Figure 5. It can be seen that the $d_{32}$ of drops is larger and fluctuates obviously during the dispersion process, and the size distribution is broad when no PVA dispersant is added. This is caused by the great dispersion resistance to turbulent force, due to a high interfacial tension between the monomer and aqueous phases and the easy agglomeration of drops in the loss of a colloidal protection to drops. It can also be seen that the $d_{32}$ and size fluctuation of drops are decreased as PVA concentration is increased from 0.2 to 2 *g/L*. When the PVA concentration is larger than 2 g/L, the $d_{32}$ and size distribution changes little as the PVA concentration is further increased.

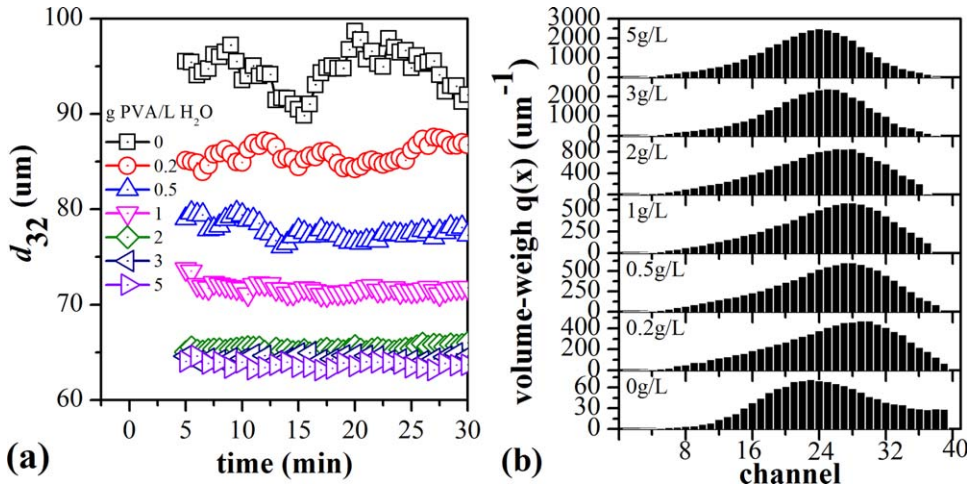


**Figure 5.** Influence of PVA dispersant concentration on $d_{32}$ (a) and size distribution (b) of MMA drops at MMA/$H_2O$ = 1/5 (mass ratio) and an agitation rate of 350 rpm. [Color figure can be viewed in the online issue, which is available at wileyonlinelibrary.com.]

**Table II.** Properties of PMMA/MMA Solution

| Concentration of PMMA (wt %) | Density ($kg/m^3$) | Viscosity (Pa s) | Interfacial tension (mN/m) |
|---|---|---|---|
| 0 | 940 | 0.000609 | 8.385 |
| 5 | 970 | 0.0310 | 4.865 |
| 10 | 987 | 0.473 | 2.405 |

The variations of $d_{32}$ and interfacial tension with PVA concentrations are shown in Figure 6. It can be seen that $d_{32}$ and interfacial tension have a similar decrease tendency as PVA concentration increased, indicating that the decrease of $d_{32}$ is mainly caused by the lowering of interfacial tension. In the liquid–liquid dispersion under the turbulent flow condition, the breakup and coalescence of drops occur continuously. The breakup of dispersed phase depends on the relative magnitude of the restoring and external deforming forces. The main external deforming forces are the turbulent pressure fluctuations and viscous stress, which keep almost unchanged at the same agitation rate. The restoring forces are mainly originated from the interfacial tension and internal viscous stress, which would be decreased as the interfacial tension between monomer and water phases decreases with the increase of PVA concentrations. Thus, the external deforming forces would be more dominant than the restoring forces, favoring the formation of smaller drops at a higher concentration of PVA dispersant.

To investigate the effects of viscosity of dispersed phase on the size and size distribution of drops in the dispersion process, PMMA/MMA solutions with different compositions were used as the dispersed phase. The physical properties of PMMA/MMA solutions and the interfacial tension between PMMA/MMA solution and water are shown in Table II. Variations of $d_{32}$ and size distribution of PMMA/MMA drops are shown in Figure 7.

As shown in Figure 7, the $d_{32}$ and size distribution breadth are smaller when pure MMA is used as the dispersed phase, while they are increased as the weight fraction of PMMA in PMMA/MMA solution or the viscosity of dispersed phase is increased. When the weight fraction of PMMA in the solution is increased to 10 wt %, $d_{32}$ is increased and the size distribution is broadened. Jahanzad *et al.*[28,47] also observed this tendency and explained by the mechanism of drop breakup shifts from bursting towards stretching as the resistance to breakup increases. Due to the wider size distribution of drops, a greater size fluctuation with time can also be seen from Figure 7.

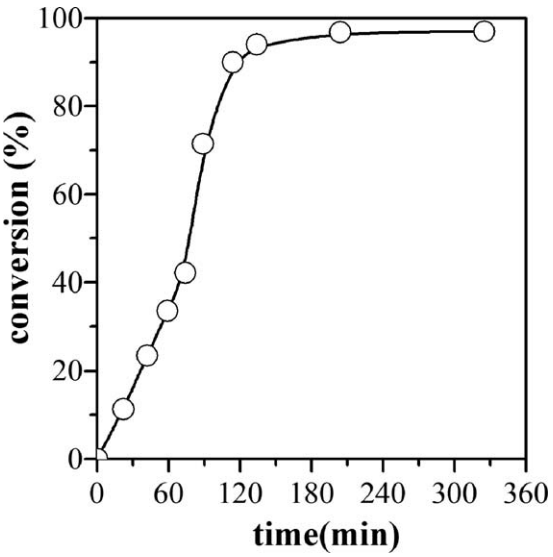


**Figure 8.** Variation of monomer conversion with time for MMA suspension polymerization at LPO = 1 wt %, PVA = 1 g/L $H_2O$, an agitation rate of 500 rpm, and a temperature of 70 °C.

### Online Monitoring of Particle Size and Size Distribution in Suspension Polymerizations

The initiator concentration and polymerization temperature were fixed in the suspension polymerizations. The typical variation of monomer conversion with time is shown in Figure 8. It can be seen that the self-acceleration of polymerization is obvious and a conversion of greater than 90% can be reached when the polymerization time exceeds 2 h.

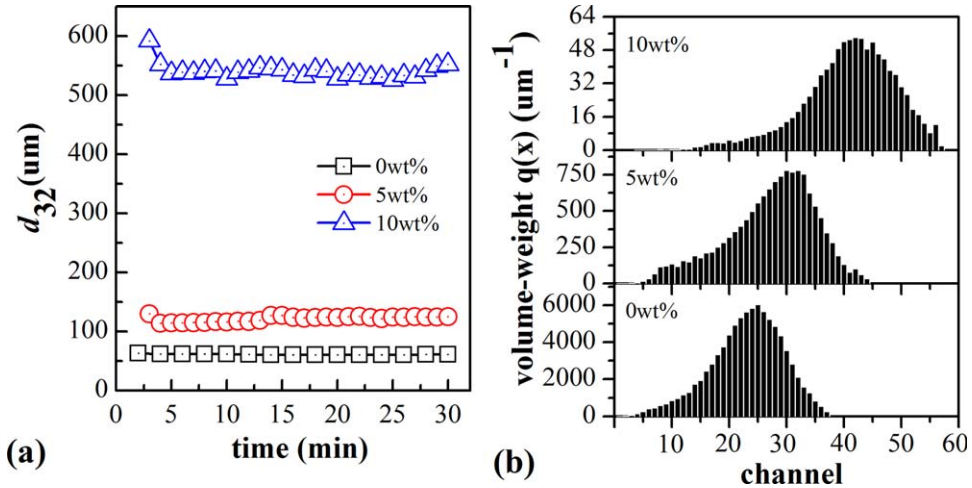


**Figure 7.** $d_{32}$ (a) and size distribution (b) of drops when using the PMMA/MMA solutions with different concentrations as the dispersed phases. [Color figure can be viewed in the online issue, which is available at wileyonlinelibrary.com.]

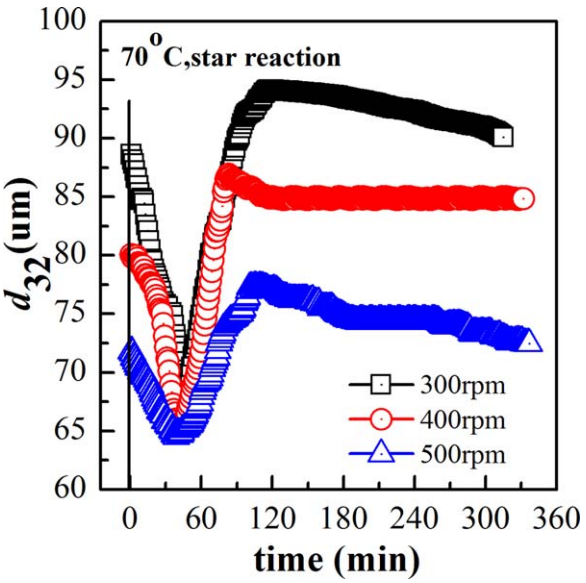


**Figure 9.** Effect of agitation rate on $d_{32}$ of particles in the suspension polymerization of MMA (LPO = 1 wt %, PVA = 1 g/L $H_2O$, 70 °C). [Color figure can be viewed in the online issue, which is available at wileyonlinelibrary.com.]

The effect of agitation rate on the variations of $d_{32}$ of particles formed in suspension polymerization is shown in Figure 9.

From Figure 9, a similar variation tendency $d_{32}$ of particles with time can be seen for suspension polymerizations conducted at different agitation rates. The $d_{32}$ is decreased at the early stage of polymerization and reaches a minimum size at about 45 min. After a short quasi-steady state, the $d_{32}$ is rapidly increased and reaches a maximum value at about 100 min. $d_{32}$ is slowly decreased at the later stage of polymerization. This variation tendency is in accord with the four characteristic particle formation intervals in the suspension polymerization, that is, the transition, quasi-steady state, growth, and identification stages. The duration of observed steady-state stage is shorter than that reported by Jahanzad *et al.*[29,47] It can also be seen that the $d_{32}$ decreases with the increase of agitation rate in all stages, because the increase of agitation rate would increase the rate of breakage and favor the formation of smaller drops when the viscosity is not too high in the transition stage. The onset of growth stage is occurred approximately at the conversion of about 25–30% and the rapid increase of particle size is closely related with the increased coalescence rate of dispersed phase, because the viscosity (and the viscous energy) of dispersed phase is increased quickly in the self-acceleration stage of polymerization. When the dispersed phase exhibits enough elasticity to balance the viscous forces with the further increase of conversion, the identification stage is achieved. The slow decrease of particle size in this stage is caused by the shrinkage as the swollen MMA monomer is converted into PMMA.

Effects of PVA dispersant concentration on the size evolutions in MMA suspension polymerization are shown Figure 10.

It can be seen that $d_{32}$ of drops/particles is decreased as the concentration of added PVA dispersant is increased at the same polymerization time. At the beginning of the reaction, the low-viscosity monomer would be broken up under the turbulent forces, while the coalescence would be minimized with the addition of PVA dispersant. As the viscosity of particles is increased, the breakage rate would decrease as the viscous forces inside the particles become greater than the turbulent forces generated by the impeller. In the sticky stage, when the colloidal protection of the dispersant to drops is not enough, the coalescence of drops would increase.[30] When the concentration of added PVA dispersant is lower, the drops with a great initial size would be formed due to the greater interfacial tension between the monomer and water phases, and the coalescence degree of drops in the growth stage would be larger since the drops with less PVA dispersant coverage are more susceptible to coalescence after

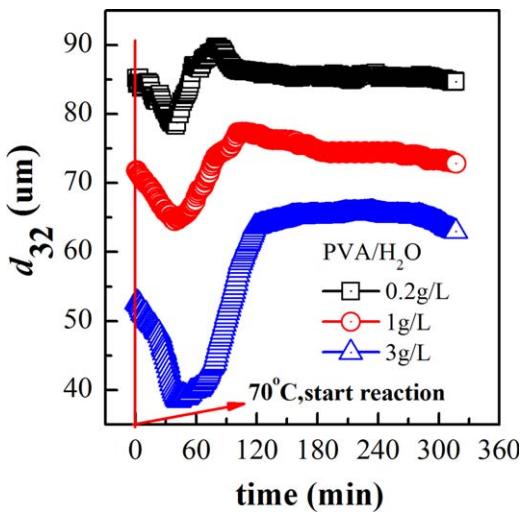


**Figure 10.** Effect of PVA concentration on variation of $d_{32}$ in MMA suspension polymerization (LPO = 1 wt %, 500 rpm, 70 °C). [Color figure can be viewed in the online issue, which is available at wileyonlinelibrary.com.]

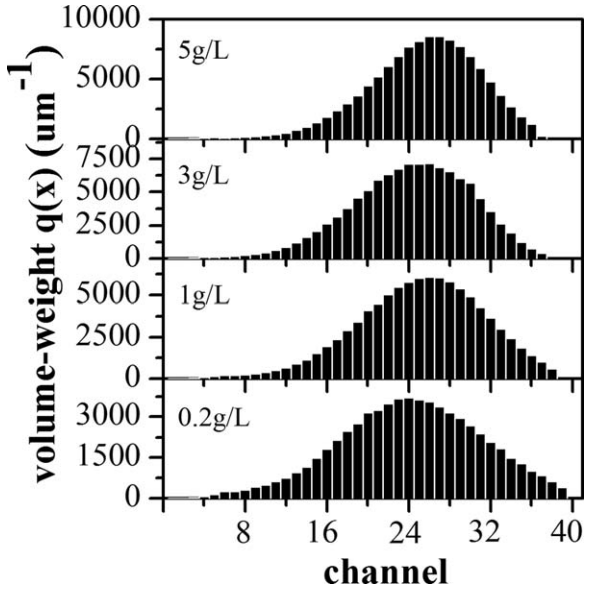


**Figure 11.** Size distribution of final PMMA particles prepared at the different PVA concentrations.

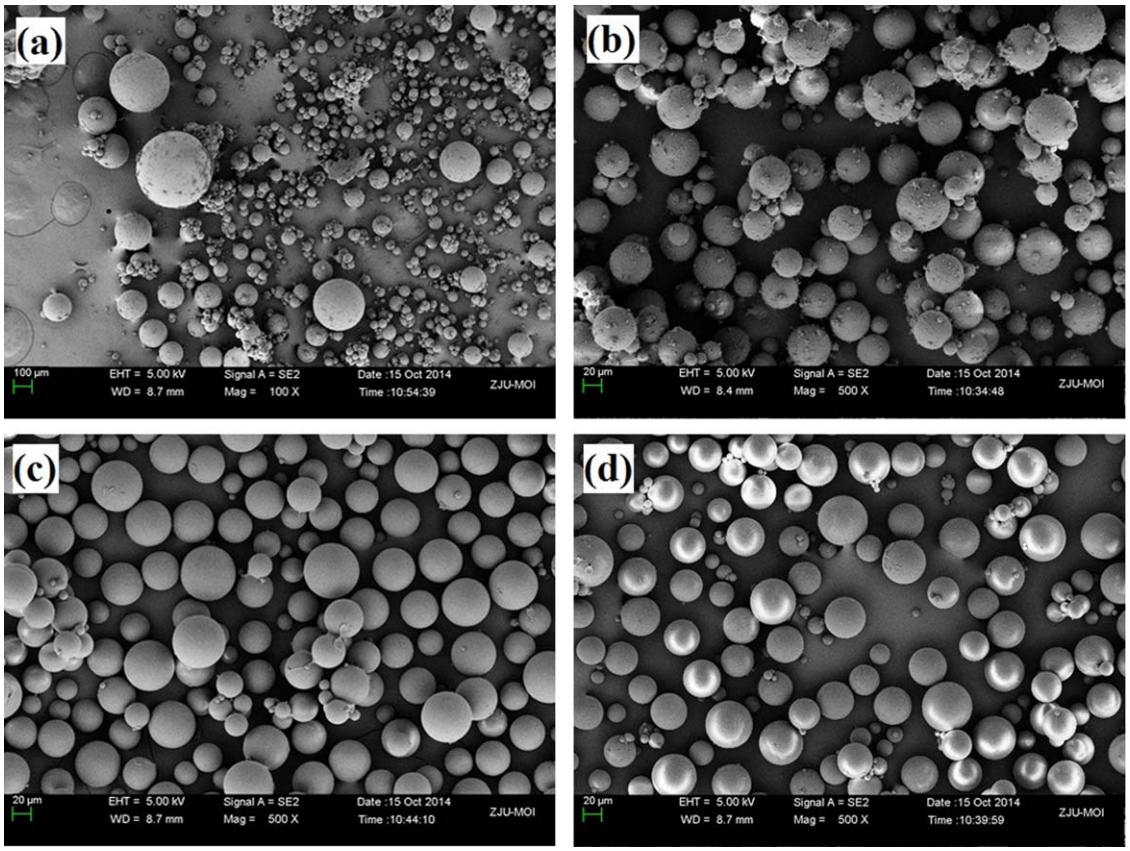


**Figure 12.** Morphology of final PMMA particles prepared at the different PVA concentrations: (a) 0.2, (b) 1, (c) 3, and (d) 5 g/L $H_2O$. [Color figure can be viewed in the online issue, which is available at wileyonlinelibrary.com.]

collision. Therefore, the size of drops/particles would be increased and the number of drops/particles would be decreased. It can also be seen that the quasi-steady-state and the growth stages are prolonged as the concentration of PVA is increased. The particle shrinkage is lower in the identification stage when the concentration of PVA concentration is higher (3 and 5 g/L).

The size distribution and morphology of final PMMA particles prepared at different PVA concentrations are shown in Figures 11 and 12, respectively.

It can be seen that the size of final PMMA particles observed by SEM is closed to that determined by ORM, and the size distribution of PMMA particles determined by ORM is also in

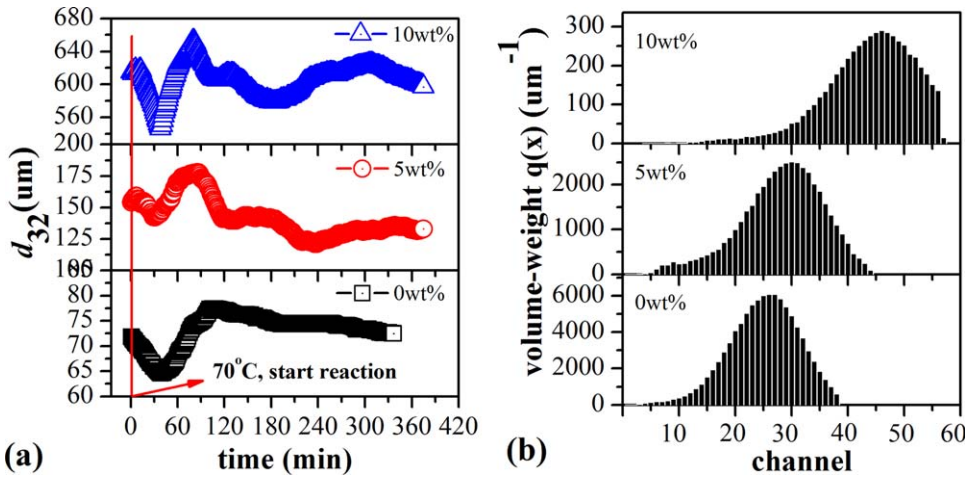


**Figure 13.** Variation of $d_{32}$ with time (a), final size distributions (b) in suspension polymerization using MMA and MMA/PMMA solutions as the initial dispersed phases (LPO = 1 wt %, PVA = 1 g/L $H_2O$, 500 rpm, 70 °C). [Color figure can be viewed in the online issue, which is available at wileyonlinelibrary.com.]

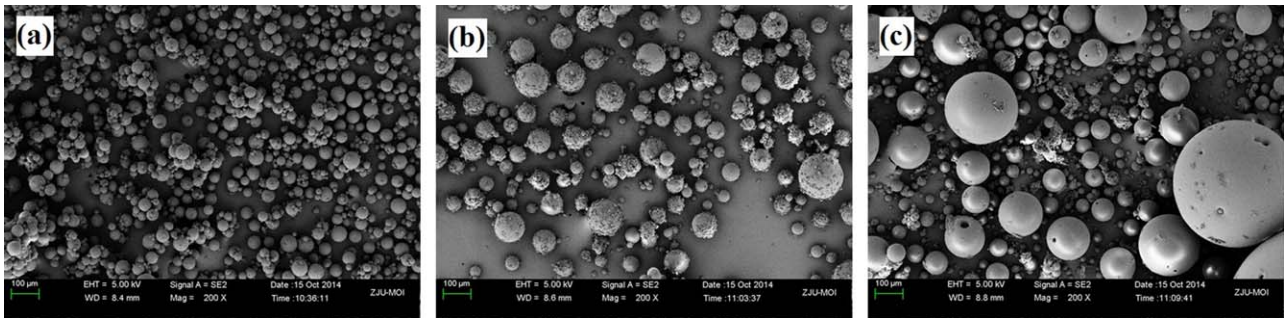


**Figure 14.** SEM micrographs of PMMA particles prepared in suspension polymerization using MMA (a) and MMA/PMMA solutions 9 (b) MMA/PMMA = 95/5, c) MMA/PMMA = 90/10] as the initial dispersed phases. [Color figure can be viewed in the online issue, which is available at wileyonlinelibrary.com.]

consistent with SEM observation. The size distribution becomes narrow as the concentration of PVA dispersant is increased. When the concentration of PVA is 0.2 g/L, the PMMA particles with both small and large sizes are formed and the size distribution is very broad. The number of small particles is significantly decreased when the concentration of PVA is increased to 1 g/L. The spherical particles with uniform sizes and smooth surfaces are formed when the concentration of PVA is further increased to 3 or 5 g/L. So, the concentration of PVA affects not only the average size, but also the size distribution and morphology of PMMA particles.

Influences of initial PMMA weight fractions (viscosities) of PMMA/MMA solutions on the variation of $d_{32}$, size distribution, and morphology of PMMA particles were also investigated and the results are shown in Figures 13 and 14.

Similar to the liquid–liquid dispersion process, the initial PMMA weight fraction of PMMA/MMA solution has a significant influence on the variations of size and size distribution of drops/particles in the suspension polymerization. When PMMA/MMA solutions containing 5 and 10 wt % PMMA are used as the dispersed phase, the quasi-steady-state and growth stages are shortened, $d_{32}$ of drops/particles are obviously increased in all stages, and the measured $d_{32}$ of particles is ceaselessly fluctuated after the growth stage. Jahanzad *et al.*[47] also observed that the steady-state stage was shortened, the growth stage was advanced, and $d_{32}$ and size distribution width was increased as the PMMA weight fraction of PMMA/MMA solution (conversion of MMA mass polymerization) increased for *in situ* mass suspension polymerization. The nonhomogeneity of turbulent flows and a change in the mechanism from bursting to stretching and erosive mechanism of drop breakup with increasing polymer content of the dispersed phase are responsible for the formation of particles with a broad size distribution. Since the breakup and coalescence are negligible after the growth stage, the fluctuation of $d_{32}$ in the identification stage of MMA suspension polymerization using PMMA/MMA solution as the dispersed phase should be attributed to the size difference of formed particles that randomly enter the laser analysis region. In other word, the fluctuation of measured $d_{32}$ reflects the wide size distribution of particles, which can also be seen from Figure 14. According to the above results, more attention should be paid to the monomer used in the industrial suspension polymerization. If the monomer contained the dissolved polymer (which may be formed during the manufacture and storage of monomer if no inhibitor is added) is directly used in suspension polymerization, the average particle size, size distribution, and morphology of the prepared polymer would be quite different from that of polymer prepared by using the pure monomer. In other case, if the agitation of suspension polymerization is accidentally stopped when polymerization has proceeded for a certain time (a certain amount of polymer has been formed), the polymer prepared by re-starting of agitation and continued suspension polymerization would also exhibit different size, size distribution and morphology from that of polymer prepared by a normal suspension polymerization process.

## CONCLUSIONS

Online ORMs were used to monitor the evolution of drop/particle size and size distribution in the liquid–liquid dispersions and suspension polymerization processes by using MMA or PMMA/MMA solutions as the model systems. The technique is reliable and sensitive to variations of average size and size distribution of drops/particles with agitation rate, PVA dispersant concentration and the composition (viscosity) of the dispersed phase. The measured $d_{32}$ of drops in liquid–liquid dispersion process was increased with the decrease of agitation rate and PVA concentration, and with the increase of PMMA weight fraction in PMMA/MMA solution. From the ORM measured variations of $d_{32}$ of particles, four characteristic particle formation stages in suspension polymerizations were confirmed. The $d_{32}$ and size distribution breadth of particles are significantly increased and the durations of quasi-steady-state and growth stages are shortened, as PVA dispersant concentration and agitation rate are decreased. The wide size distribution of drops/particles was reflected by the significant fluctuation of $d_{32}$ when the concentration of added PVA dispersant was lower (i.e., <0.2 g/L $H_2O$) or MMA/PMMA solutions containing 5 and 10 wt % PMMA was used as the dispersed phase. Thus, to obtain the PMMA particles with a narrow size distribution in the industrial suspension polymerization, a relatively higher concentration of dispersant and the monomer containing no polymer should be used.

## NOMENCLATURE

| | |
|---|---|
| $d_{32}$ | Sauter mean diameter (μm) |
| $Q_r$ | the cumulative frequency |
| $x$ | the characteristic parameter value of particle |
| $q_r(x)$ | density distribution ($\mu m^{-1}$) |
| $K_1$, $K_2$ | constants of proportionality |
| $D$ | impeller diameter (m) |
| $N$ | agitation rate (rpm) |
| $We$ | Weber number, $\rho_c N^2 D^3/\sigma$, (dimensionless) |

## REFERENCES


1. Yuan, H. G.; Kalfas, G.; Ray, W. H. *J. Macromol. Sci. Part C: Rev. Macromol. Chem. Phys.* **1991**, *C31*, 215.
2. Vivaldo-Lima, E.; Wood, P. E.; Hamielec, A. E. *Ind. Eng. Chem. Res.* **1997**, *36*, 939.
3. Brooks, B. W. *Chem. Eng. Technol.* **2010**, *33*, 1737.
4. Hinze, J. O. *AIChE J.* **1955**, *1*, 289.
5. Shinnar, R.; Church, J. M. *Ind. Eng. Chem.* **1960**, *52*, 253.
6. Leng, D. E.; Quarderer, G. *J. Chem. Eng. Commun.* **1982**, *14*, 177.
7. Lee, J. M.; Soong, Y. *Ind. Eng. Chem. Process Des. Dev.* **1985**, *24*, 118.
8. Calabrese, R. V.; Chang, T.; Dang, P. T. *AIChE J.* **1986**, *32*, 657.
9. Wang, C. Y.; Calabrese, R. V. *AIChE J.* **1986**, *32*, 667.
10. Lagisetty, J. S.; Das, P. K.; Kumar, R. *Chem. Eng. Sci.* **1986**, *41*, 65.
11. Hashim, S.; Brooks, B. W. *Chem. Eng. Sci.* **2002**, *57*, 3703.
12. Hashim, S.; Brooks, B. W. *Chem. Eng. Sci.* **2004**, *59*, 2321.
13. Zerfa, M.; Brooks, B. W. *Chem. Eng. Sci.* **1996**, *51*, 3223.
14. Zerfa, M.; Brooks, B. W. *Chem. Eng. Sci.* **1996**, *51*, 3591.
15. Konno, M.; Arai, K.; Saito, S. *J. Chem. Eng. Jpn.* **1982**, *15*, 131.
16. Isopescu, R.; Postelnicescu, P.; Palau, R.; Dumitrescu, A.; Josceanu, A. M. *Chem. Eng. Trans.* **2010**, *21*, 943.
17. Maggioris, D.; Goulas, A.; Alexopoulos, A. H.; Chatzi, E. G.; Kiparissides, C. *Chem. Eng. Sci.* **2000**, *55*, 4611.
18. Chatzi, E. G.; Boutris, C. J.; Kiparissides, C. *Ind. Eng. Chem. Res.* **1991**, *30*, 536.
19. Chatzi, E. G.; Boutris, C. J.; Kiparissides, C. *Ind. Eng. Chem. Res.* **1991**, *30*, 1307.
20. Jahanzad, F.; Sajjadi, S.; Brooks, B. W. *Ind. Eng. Chem. Res.* **2005**, *44*, 4112.
21. Boscher, V.; Helleboid, R.; Lasuye, T.; Stasik, B.; Riess, G. *Polym. Int.* **2009**, *58*, 1209.
22. Alban, F. B.; Sajjadi, S.; Yianneskis, M. *Chem. Eng. Res. Des.* **2004**, *82*, 1054.
23. Santos, J. G. F.; Way, D. V.; Melo, P. A.; Nele, M.; Pinto, J. C. *Macromol. Symp.* **2011**, *299/300*, 57.
24. Santos, A. F.; Lima, E. L.; Pinto, J. C. *J. Appl. Polym. Sci.* **2000**, *77*, 453.
25. Santos, A. F.; Lima, E. L.; Pinto, J. C. *J. Appl. Polym. Sci.* **1998**, *70*, 1737.
26. Santos, J. C.; Reis, M. M.; Machado, R. A. F.; Bolzan, A.; Sayer, C.; Giudici, R.; Araújo, P. H. H. *Ind. Eng. Chem. Res.* **2004**, *43*, 7282.
27. Lazrak, N.; Le Bolay, N.; Ricard, A. *Euro. Polym. J.* **1998**, *34*, 1637.
28. Jahanzad, F.; Sajjadi, S.; Brooks, B. W. *Macromol. Symp.* **2004**, *206*, 255.
29. Jahanzad, F.; Sajjadi, S.; Brooks, B. W. *Chem. Eng. Sci* **2005**, *60*, 5574.
30. Goncalves, O. H.; Nogueira, A. L.; Araújo, P. H. H.; Machado, R. A. F. *Ind. Eng. Chem. Res* **2011**, *50*, 9116.
31. Simmons, M. J. H.; Zaidi, S.; Azzopardi, B. *J. Opt. Eng* **2000**, *39*, 505.
32. McDonald, K. A.; Jackman, A. P.; Hurst, S. *Biotechnol. Lett.* **2001**, *23*, 317.
33. Jeffers, P.; Raposo, S.; Lima-Costa, M.; Connolly, P.; Glennon, B.; Kieran, P. M. *Biotechnol. Lett.* **2003**, *25*, 2023.
34. Barrett, P.; Glennon, B. *Inst. Chem. Eng.* **2002**, *80*, 799.
35. Cull, S. G.; Lovick, J. W.; Lye, G. L.; Angeli, P. *Bioproc. Biosyst. Eng.* **2002**, *25*, 143.
36. Lovick, J.; Mouza, A. A.; Paras, S.; Lye, G. J.; Angeli, P. *J. Chem. Technol. Biotechnol.* **2005**, *80*, 545.
37. Maaß, S.; Wollny, S.; Voigt, A.; Kraume, M. *Exp. Fluids* **2011**, *50*, 259.
38. Heinrich, J.; Ulrich, J. *Chem. Eng. Technol.* **2012**, *35*, 967.
39. Poblete, I. B.; Castor, C. A.; Nele, M.; Pinto, J. C. *Macromol. Symp.* **2014**, *344*, 94.
40. Sommer, K. *Part. Part. Syst. Char.* **2001**, *18*, 22.
41. Jahanzad, F. Evolution of Particle Size Distribution in Suspension Polymerisation Reactions; Ph.D. Thesis, University of Loughborough, Loughborough, May **2004**.
42. Zhou, G.; Suzanne, K. *Chem. Eng. Sci.* **1998**, *53*, 2063.
43. Zainal Abidin, M. I. I.; Abdul Raman, A. A.; Mohamad Nor, M. I. *Ind. Eng. Chem. Res.* **2014**, *53*, 6554.
44. Pacek, A. W.; Man, C. C.; Nienow, A. W. *Chem. Eng. Sci.* **1998**, *53*, 2005.
45. Desnoyer, C.; Masbernat, O.; Gourdon, C. *Chem. Eng. Sci.* **2003**, *58*, 1353.
46. Coulaloglou, C. A.; Tavlarides, L. L. *AIChE J.* **1976**, *22*, 289.
47. Jahanzad, F.; Sajjadi, S.; Yianneskis, M.; Brooks, B. W. *Chem. Eng. Sci.* **2008**, *63*, 4412.